Sensitivity analysis of Seawater intrusion model in Tra Vinh province, Mekong Delta

xuan xie (2535877992@qq.com)
Personal Growth Institute https://orcid.org/0000-0002-6662-0478
li yu ke
TUDelft: Technische Universiteit Delft

Research Article

Keywords: coastal aquifers, groundwater flow and salinity transport model, seawater intrusion, sensitivity analysis

Posted Date: August 10th, 2021

DOI: https://doi.org/10.21203/rs.3.rs-748535/v1

Abstract

Seawater intrusion into coastal aquifers is a serious problem, leading to shortage of water supply in Tra Vinh province which is a typical coastal province in Mekong Delta Vietnam. One of the main reason for salinity intrusion is excessive abstraction from groundwater. In addition, climate change is an uncertain challenge which may affect the situation in the future. GMS groundwater modelling is an effective tool to simulate groundwater flow and salinity transport processes in this research. A conceptual and numerical model were built and calibrated to simulate groundwater flow in the case study area located in Tra Vinh with the use of hydraulic head data accumulated in the period 2006 to 2017, a sensitive analysis has been conducted on hydraulic conductivities, specific storage and conductance of boundary condition in order to understand model behaviour. Model results show that groundwater is overexploited in Tra Vinh province. Groundwater levels were continuously decreased in the whole area and in all aquifers. Groundwater recharge is limited due to impermeable layers on surface and is recharge is only possible in sand dune areas. Groundwater abstraction supplies domestic water demand which is much more than recharge. The sensitivity analysis shows that hydraulic conductivity is the most sensitive factor impacting the vales of the groundwater heads. Hydraulic conductance of the boundary is the most sensitive parameter under the head-dependent flow boundary, and hydraulic conductivity is the least sensitive parameter. However, specific storage is more sensitive to impact the values of change of storage. Thus, Boundary conductance, hydraulic conductivity and specific storage coefficient are important parameters for the accuracy of the model results. Saline groundwater occurs in the coastal zone and in the north area. Saltwater intrusion occurs in these area. The salinity data availability is too limited to provide a clear description of salinity distribution in the area.

1. Introduction

Groundwater resources are important freshwater resources which are often used as drinking water, agricultural water and industrial water in most of regions (Vengadesan and Lakshmanan 2019). Coastal areas belong to one of the richest environment of agriculture, industry and fishery, more than half of the word’s mega-cities lie within 50 km of the coast, and population densities here are 2.6 times greater than island (Montagna 2013), so population is often dense in coastal areas (McLusky and Elliott 2004, Wolanski and Elliott 2015, Dang 2019). Dense population, agricultural and industrial activities demand a lot of freshwater in costal zones, while fresh surface water was polluted, effected by climate change and overexploitation (Post 2005). Groundwater resources often are the main freshwater resources in most of costal resigns, but groundwater resources are vulnerable to human activities and climate change especially in coastal area(Unsal 2014, Michael 2017).

Demands of freshwater is increasing because of population growth and economic development. Fresh groundwater is excessively abstracted in coastal regions due to a growth in water demanding activities. Aquifers of coastal regions connect fresh groundwater in fields to sea water (Janardhanan 2012). Excessive exploitation of groundwater results in some negative consequences such as seawater

migrating into aquifer systems which is called as saltwater intrusion, increased freshwater pollution and influences for local ecosystem (Post and Werner 2017).

Saltwater intrusion obviously affects the quality of the groundwater, over 1% of seawater (250 mg/l chloride) turns fresh water in unsuitable drinking purpose (Werner 2013). Not only overexploitation but also global warming which cause sea level raise and other climate change impacts affects the groundwater quality (Janardhanan 2012).

Simulating saltwater intrusion with the use of groundwater flow and salinity transport model is challenging, so sensitive analysis have important significant to model calibration and provide recommendation for data collection (Razavi 2015). Sensitivity analysis can help to analysis the robustness of the model and simplify model (Pannell 1997, Saltelli, Ratto et al. 2008). few sensitive analysis studies addressed parameter sensitives in saltwater intrusion modelling process. Shoemaker (2004)reported that dispersivity is important parameter to simulating and observing hydraulic head and salinity through parameter sensitives analysis for SEAWAT model (Shoemaker, W. B 2004).

In this study, the major challenge is simulating groundwater flow and salinity transport process. Output of the GMS model is variable because of the varying input factors during the simulation process. But the model which we need is an accurate simulation between model's output and real-word phenomena. Parameter sensitives are applied to calibrating and assess the model and improve models input value to obtain more accurate model. meanwhile the study aims to conduct an in-depth analysis of factors affecting model accuracy in Tra Vinh province. This research include follow steps. 1. model setup, conceptual model adjusting, numerical model construction, and model calibration. 2. Sensitive analysis for parameters. 3. Discussing the results of parameters sensitivity analysis. 4. Conclusion through analysing results.

2. Material And Methods

GMS is an integral groundwater modelling environment, it is often used to simulate and construct groundwater models, for instance groundwater flow, groundwater transport and salinity intrusion models. GMS provides pre- and -post processors for MODFLOW, SEAWAT and MT3DMS which are needed to be used in the research.

The GMS model has been built to evaluate the condition of groundwater abstraction and salinity intrusion in Tra Vinh province. Salinity intrusion as the main problem limiting groundwater development. Groundwater flow and saltwater transport models were chosen to assess groundwater conditions. In order to simulate groundwater system with the use of GMS tools, some basic steps are necessary in GMS modelling process.

2.1 Research site

The Mekong river flows into the sea through a number of branches (Hoc 2005). Mekong Delta is located in the southwestern of Vietnam the downstream of the Mekong River. It is a very flat area. Tra Vinh province is located in Mekong delta costal resign, which is separated with other province by Co Chine River (boundary between Ben Tre, Vinh Long and Tra Vinh province on the north) and Hau River (boundary between Soc Trang and Tra Vinh province on the west). On the east of Tra Vinh province is the East Sea with 65km costal line (Thu 2007). The province is a lowland costal area, the elevation of this area is only 0.5-1m above sea level (Nguyen 2000).

The area of Tra Vinh is about 2215.1km2, there are about 1.1 million inhabitants live there. Population density is about 460/km2 (Nguyễn 2011). It comprises one provincial capital city (Tra Vinh) and seven districts (Cang long, Chau Thanh, Cau Ke, Tieu Can, Cau Ngang, Tra Cu and Duyen Hai). The topography is very complex, as there are hundreds of mounds and sand caves, alluvial deposits, coastal plain and complex network of rivers and cannels in Tra Vinh province show in figure1.

Sea transgression and regression formed and developed Mekong Delta in Quaternary period (Chiem 1993). The soil is deposited by floods from the rivers and sea in this delta, meanwhile different particles of sediment deposited in different area which cause distribution of different soil textures in different areas (Ve 1990). The type of soil is an important factor which determine the use of land in Vietnam (Postma 2007).

There are three major soil types in Tra Vinh (1) sandy soil; (2) alluvial land; and (3) acidic soil (Nguyen 2020). Figure 2 shows the map of soil types in Tra Vinh province.

Nowadays, people abstract groundwater to supply daily life, industries production and irrigate agriculture in Tra Vinh (Ha 2015). Meanwhile the demands of fresh groundwater are increasing due to climate change, urbanization, social-economic development and population density growth in Tra Vinh (Danh 2008). So excessive groundwater extraction for different usages is a serious problem in Mekong Delta, especially in Tra Vinh province which is a typically coastal province of Vietnam in Mekong Delta (Minh 2014). The abstraction of groundwater volume is about 347,793m3/d in 2016 in Tra Vinh, it could increase in the future (Van 2017, Van Hiep 2018).

As time goes by, the balance between abstraction and recharge in coastal aquifer is disturbed due to overexploitation. This leads to groundwater level decrease and salinity intrusion in Tra Vinh (Vermeulen 2013). On the other hand, coastal aquifers are vulnerable to seawater intrusion. This problem is also caused by sea level rise which is triggered by global warming. The quality effects on valuable groundwater resources results in a shortage of water availability and other serious damages (Nguyen 2014). Seawater intrusion threatens nearly 38000 hectares of cultivated rice field every year in Tra Vinh (Herrera-Pantoja and Hiscock 2008), it has also caused fresh water shortages in people daily life and economic development.

2.2 Construction of conceptual model

The domain of the model is for the whole Tra Vinh province which is about 2215.1 km2. Groundwater abstraction data, recharge and hydraulic data from 2007 to 2016 was put into GMS model to simulate groundwater flow process under the GIS map in Tra Vinh province. A hydrogeological conceptual model has been built to describe basic characteristics of groundwater system. It is the basic of for creating numerical models such as MODEFLOW, MT3DMS and SEAWAT. The conceptual model include: Aquifer structures; Boundary conditions; Hydrogeological parameters; Hydrological stresses and observations. the situation of observation wells show in table1.

2.3 numerical model

Groundwater flow models are normally used to simulation the hydraulic flow patterns process with the use of three-dimensional model. MODFLOW is the most commonly used software in numerical groundwater flow models with the use of finite different method. MODFLOW is applied in groundwater simulation process, aiming to solve unsustainable problems and then optimize system process. The partial differential equation is the base of MODFLOW for confined aquifer (McDonald and Harbaugh 1988). It is:

$$\frac{\partial}{\partial x}\left(K_{xx}\frac{\partial h}{\partial x}\right)+\frac{\partial}{\partial y}\left(K_{yy}\frac{\partial h}{\partial y}\right)+\frac{\partial}{\partial z}\left(K_{zz}\frac{\partial h}{\partial z}\right)-W=S_s\frac{\partial h}{\partial t} \qquad (1)$$

Where $K_{xx}K_{yy}K_{zz}$ are values of hydraulic conductivity along x, y and z coordinate axes, all of these are assumed to be parallel to the major axes of hydraulic conductivity (Lt-1); h is the groundwater head (L); W is a volumetric flux per unit volume and represents sources and sinks of water (t-1); Ss is the special storage of the porous material (L-1); t is the time (t).

MT3DMS is multi-species and three-dimensional transport model for simulation of groundwater systems which include advection, dispersion and chemical reaction of dissolved constituents process, it is evolved from MT3D (Zheng and Wang 1999).

MT3DMS linked with MODFLOW, it uses hydrologic and discretization features of MODFLOW which support the flow solution which is required through the transport simulation process. The governing equations in MT3DMS is (Zheng and Wang 1999):

$$\frac{\partial(\theta C^k)}{\partial t}=\frac{\partial}{\partial x_i}\left[\theta D_{ij}\frac{\partial C^k}{\partial x_j}\right]-\frac{\partial}{\partial x_i}(\theta v_i C^k)+q_s C_s^k+\sum R_n \qquad (2)$$

Where Ck is the dissolved concentration of species k, ML-3; θ is the porosity of the subsurface medium, dimensionless;t is the time, T; xi is the distance along the respective Cartesian co-ordinate axis, L; Dij is the hydrodynamic dispersion coefficient tensor, L2T-1; vj is the seepage or linear pore water velocity, LT-1; It is related to the specific discharge or Darcy flux through the relationship v= qi/θ; qs is the volumetric flow rate per unit volume of aquifer representing fluid sources (positive) and sink (negative), T-1; Csk is

the concentration of the source or sink flux for species k, ML-3; $\sum$Rn is the chemical reaction term, ML-3T-1.

Darcy's law connect transport equation with flow equation, it is:

$$v_i = \frac{q_i}{\theta} = -\frac{K_i}{\theta}\frac{\partial h}{\partial x_i} \quad (3)$$

Where K_i is principal component of the hydraulic conductivity tensor, LT-1; h is hydraulic head which can be calculated from the 3D groundwater flow equation, L.

2.4 Set-up of numerical models

A numerical groundwater flow model was built. The model consisted of 135 rows and 151 columns with a constant cell size of 500m x 500m grids, and included 13 layers that consist of 7 aquifers and 6 aquitards.

In the new model, each of 6 confined aquifers were divided into two model layers. The top unconfined aquifer and 6 aquitards were still simulated with one mode layer since they are very thin. In total, 19 model layers were included in the model. Stress period is defined one month length and 121 stress periods were set up from 2006 to 2017 which was similar with old model.

The main step to rebuild the numerical model are in follow:

1. a grid frame was created to cover the same model area which has a dimension of length is x as 75000, length in y as 67000.

2. the old model grid data was saved and converted to 2D scatter data sets to be used to provide top and bottom elevations and starting heads for the new model.

3. a new 3D grid was created with the model refinement which consisted of 750 rows, 670 columns and 19 layers. Then, a new MODFLOW model was constructed with the new model grid. The top and bottom elevations and starting heads of the new model were interpolated from the 2D scatter data sets of the old model.

4. the conceptual model was revised according to 19 model layers. Nineteen coverages of hydrogeological parameters were created, abstraction wells were redistributed to new aquifer layers, observation wells were assigned to new aquifer layers. The lateral boundaries in the north, east, and west of the aquifer layers were defined as head-dependent flow boundaries and were simulated with MODFLOW General Head Boundary (GHB) package. The coastal line was simulated by two different boundary conditions: head-dependent flow boundary (GHB) and a constant head boundary. The results were compared in sensitivity analysis.

5. the data defined in the conceptual model was transferred into MODFLOW model by automatic mapping and conversion tool in GMS. Table 2 provides the link between GMS conceptual model coverage and MODFLOW packages.

6. MODFLOW model was run to compute transient groundwater levels and flow budgets. The computed levels were checked with observed values.

7. a new MT3DMS model was constructed with the new grid, and cell-by-cell flow component generated by MODFLOW. Starting concentrations distribution in space were defined the same with old model. Meanwhile third order TVD scheme technique was choose to solve the advection terms under MT3DMS Advection Package.

8. the data defined in the conceptual model was transferred into MT3DMS model by mapping, then running MT3DMS model to compute transient total dissolved solid concentration, the computed values were checked with observed values.

9. new SEAWAT model was constructed based on MODFLOW and MT3DMS model, then transient salinity intrusion results were generated.

2.5 Numerical model calibration

The transient groundwater flow and transport model were calibrated through comparing the observed values and computed values, hydrogeological parameters were adjust to achieve the best simulation between calculated and observed groundwater head values. Calibration aimed at layers 1, 3, 13 and 19, because there are a big error between observed and computed groundwater head and salt concentration.

Manual calibrated was used in this research, the accuracy of the calibration was checked with statistic indicators: mean error (ME), root mean squared error (RMSE) and Standard Deviation.

2.6 Sensitivity analysis

Advection package play an important role in MT3DMS simulation process, there are some solution schemes that can be divided into three major techniques which can used to solve transport equation in this package. i.e., standard finite different method, higher-order finite-volume TVD method and partial tracking based Eulerian-Lagrangian methods.

Dispersion and sink mixing package are also main packages to solve the concentration change due to dispersion with explicit finite different method and fluid sink mixing with the explicit finite different method separately.

Sensitive analysis was carried through adjusting the hydraulic conductivity, specific storage, boundary conductance and with the use of GHB boundaries.

The hydraulic conductivity values from the calibrated model were used as benchmark values. The hydraulic conductive values of all aquifer layers were increased by 50% and decreased by 50% systematically, The output data were different by increasing 50% and decreasing 50% of hydraulic conductivities values (changing K_h and K_v at same time). The computed groundwater levels and water budgets were computed with values from the benchmark values to show sensitivity of groundwater levels and budget to hydraulic conductivity.

In the same way, sensitivity of specific storage was checked by increasing 50% and decreasing 50% of the benchmark values.

The sensitivity of the boundary conditions were checked under two different coastal line boundary: head-dependent flow boundary and constant head boundary.

The lateral boundary of north, west and east were simulated with: head-dependent flow boundaries. The amount of water flow through the boundaries is controlled by the conductance values as defined as (McDonald and Harbaugh 1988):

$$G_{arc} = KW\frac{L}{D} \qquad (4)$$

Where K is the average hydraulic conductivity; W is the thickness of the saturated aquifer perpendicular to the flow direction; L is the boundary length perpendicular to the flow direction; D is the distance from the general head boundary to the model boundary

The conductance values were also increased and decreased by 50% of the benchmark values to check the influences of boundaries. When the coastal line was simulated by general head boundary, the conductance was also changed accordingly. When the coastal lime was simulated by constant head boundary, only conductance of other boundaries were changed.

3. Results

3.1 Model calibration

The transient MODFLOW model was calibrated by try and error method. Hydraulic conductivities and abstraction rates were adjusted in order to get the better fit of calculated and observed groundwater head. The plot of calculated groundwater head and observed groundwater head in wells Q07701H (layer 1and Q021050 (layer 19) are shown in Figure 3.

The contour map of groundwater head in layer 1(Holocene (qh)) layer 4 (Upper Pleistocene (qp_3)) layer 7 (Upper-Middle Pleistocene (qp_{2-3})) in 1/1 2017 are shown in the Figure 4.

The water budget for the whole model are shown in Figure 5. The groundwater abstraction as the main outflow of groundwater has increased, and changes of the groundwater storage have decreased from

2006 to 2017. Meanwhile changes of the groundwater storage and recharge from top unconfined aquifer which as the main inflow source of groundwater have the same trend in each stress periods. The boundary inflow slowly rises and is an important source of the groundwater storage. River leakage has a little effect on the groundwater storage.

SEAWAT was run to check TDS variations in space and on time. Currently, the SEAWAT model could not be calibrated due to lack of long-term continuous measurements of the concentration. The plot of calculated TDS and observed TDS in the observation wells Q07701H (layer 1) are shown in Figure 6.

The contour map for total dissolved solid (TDS) in layer 1 (Holocene (qh)) layer 4 (Upper Pleistocene (qp_3)) and layer 7 (Upper-Middle Pleistocene (qp_{2-3})) in 1/1 2017 are shown in Figure 7.

3.2 Sensitive analysis of parameters

3.2.1 influences of Hydraulic conductivities

Groundwater head results in each stress periods in wells Q07701H (layer 1), Q404020 (layer 4), Q40403T (layer 7), Q40403Z (layer 13), Q2017040 (layer 16) and Q021050 (layer 19) are shown in Figure 8. The mean computed groundwater head and difference between previous and new results of K values of $0.5K_0$ and $1.5K_0$, are shown in Table 3.

Groundwater levels in different aquifers react differently on the changes of hydraulic conductivities as shown in Figure 8. In the top unconfined aquifer, groundwater level decreases when the hydraulic conductivity increases since more water will flow downwards to lower aquifers through leakage (Q07701H (layer 1)). Groundwater levels in lower confined aquifers increase when the hydraulic conductivity increases since confined aquifers receive the leakage from the top aquifer. The magnitude of groundwater levels changes comparing to the benchmark values (k_0) is presented in Table 3. The relative changes of groundwater levels are higher when the hydraulic conductivity values are decreased by 50%.

The water budget has a strong relation with the hydraulic conductivities, especially the boundary inflow and the change of storage. The boundary inflow results with the use of different K values and the difference between each situations in Tra Vinh are shown in Figure 9 and Table 4, respectively.

Changes of the hydraulic conductivities have slight influence on the boundary inflow as shown in figure 9. The boundary inflow increases when the hydraulic conductivity increases since more water will inflow the model domain through boundaries. The changes of the boundary inflow compared to the benchmark values (k_0) are shown in Table 4. The comparative changes of the boundary inflow are higher when the hydraulic conductivity values increase with 50%. ues are decreased by 50%.

The change of storage is also impacted by changes of the hydraulic conductivities as shown in Figure 10. Change of storage increases when the hydraulic conductivity increases since more water will be stored in the aquifers. The change of storage of $0.5k_0$ and $1.5k_0$ comparing to the one of benchmark

values (k_0) is shown in Table 5. The relative change of storage is higher when hydraulic conductivity values are increased by 50% ($1.5k_0$).

3..2.2 influences of Storage coefficients

The storage coefficient is also one of the important factors which has significant impact on the model output values. The output data were different by increasing 50 percent and decreasing 50% of the specific storage values (Ss). The groundwater head results in each stress periods in wells Q07701H (layer 1), Q404020 (layer 4), Q40403T (layer 7), Q40403Z (layer 13), Q2017040 (layer 16) and Q021050 (layer 19) are shown in Figure 11. It is shown in Table 6 with the mean computed groundwater head and difference between new results of Ss values changes into 0.5 Ss0, 1.5 Ss_0 and previous results in 11 wells.

The groundwater levels in different aquifers react differently on the changes of specific storage coefficients as shown in Figure 11. Groundwater level in aquifers increases when the specific storage coefficients increases since more water will storage in aquifers. The magnitude of changes of groundwater levels comparing to the benchmark values (Ss_0) is presented in Table 6. The relative changes of groundwater levels are small in each aquifers when the hydraulic conductivity values are decreased by 50% or increased by 50%.

Changing of specific storage have obvious influences on boundary inflow is shown in Figure 12. Boundary inflow increase when the specific storage change 50% since more water will inflow the model domain through boundaries. The change of boundary inflow comparing to the benchmark values is shown in Table 7 The comparative changes of boundary inflow are higher when hydraulic conductivity values are decreased by 50%.

Change of storage is also impacted by changes of specific storage shown in Figure 13. Change of storage increase when the specific storage changed by increased 50% and decreased 50% since more water will storage in aquifers. The varying of change of storage comparing to the benchmark values (Ss_0) is shown in Table 8. The relative change of change of storage is higher when specific storage values are decreased by 50%.

3.2.3 influences of Boundary conductance

Output data were different by increasing 50% and decreasing 50% of conductance values of general head boundary (C_{ghb0}). Groundwater head result in each stress periods in wells Q07701H (layer 1), Q404020 (layer 4), Q40403T (layer 7), Q40403Z (layer 13), Q2017040 (layer 16) and Q021050 (layer 19) were shown in Figure 14. The mean compute groundwater head and different between new results which C_{ghb0} values are changed into 0.5 C_{ghb0} and 1.5 C_{ghb0} and previous results in 11 wells can be seen in Table 9.

Groundwater levels in different aquifers react on the changes of boundary conductance as shown in Figure 14. Groundwater level increases when the boundary conductance increases since more water will

flow downwards to aquifers through recharge and leakage from different boundaries. The magnitude of changes of groundwater levels comparing to the benchmark values (C_{ghb0}) is presented in Table 9. The relative changes of groundwater levels are higher when the boundary conductance values are decreased by 50%.

Changing of boundary conductance have great influences on boundary inflow is shown in Figure 15. Boundary inflow increases when the boundary conductance increases since more water will inflow the model domain through boundaries. The change of boundary inflow comparing to the benchmark values (C_{ghb0}) is shown in Table 10. The comparative change of

Change of storage is also impacted by changes of boundary conductance shown in Figure 16. Change of storage increase when the boundary conductance increase since more water will storage in aquifers through boundary. The varying of change of storage comparing to the benchmark values (C_{ghb0}) is shown in Table 11. The relative change of change of storage is higher when boundary conductance values are decreased by 50%. boundary inflow are higher when boundary conductance values are decreased by 50%.

3.2.4 Groundwater head sensitive to different parameters

Groundwater levels were affected by adjusting hydraulic conductivity, specific storage coefficient, and conductance of boundaries. Hydraulic conductivity as a measurement for the difficulty of water flows through sediments is the most sensitive parameter for groundwater levels. Groundwater levels in different aquifers changes from 0.3 to 4.5m by decreasing or increasing 50% of hydraulic conductivity, and it just changes from 0.06 to 0.5m and 0.1 to 0.6m for adjusting 50% of specific storage values and boundaries conductance values separately. But groundwater levels in different aquifers have different sensitivity for hydraulic conductivity. Groundwater levels in lower confined aquifers are more sensitive than the top unconfined aquifer and the changes of top unconfined aquifer are below 0.5m and it is over 1m in lower aquifers. The major reason is that recharge happened in unconfined aquifer which caused that groundwater resilience in top unconfined aquifer is higher than the one in lower confined aquifers. Accuracy of hydraulic conductivity is exact significant to obtain accurate groundwater levels.

3.2.5 Boundary inflow sensitive to different parameters

Boundary inflow is also a significant observed values to sensitive analysis for hydraulic conductivity, specific storage and boundary conductance. The most sensitive parameter for boundary inflows in the whole model domain is boundary conductance. The change of boundary inflow by increasing 50% of boundary conductance is about 10000 m^3/day, but there are only nearly 500 m^3/day and 1600 m^3/day of change by increasing 50% for hydraulic conductivity and specific storage, separately. Comparing with change of about 24 m^3/day and 6800 m^3/day by decreasing 50% hydraulic conductivity and specific storage values respectively, there is a change of more than 15000m^3/day by decreasing 50% of boundary conductance. The reason might be that conductance is more directly factor than hydraulic conductivity

and specific storage to impact the boundary inflow. In order to get reasonable boundary inflow values, it is suitable to adjust boundary conductance values closer to the real.

3.2.6 Change of storage sensitive to different parameters

The changes of hydraulic conductivity, specific storage and boundary conductance also have different influences towards change of storage values. Change of storage is more sensitive to specific storage, sensitive to increase of hydraulic conductivity when increase 50% of hydraulic conductivity the different between changed change of storage and benchmark change of storage values is trend 5000 m^3/day, but it trend to zero when decrease hydraulic conductivity by 50% . And it is less sensitive to boundary conductance, the different between changed boundary conductance values and benchmark values are trend to zero. Both hydraulic conductivity and specific storage coefficient are important for further precise storage values change.

4. Conclusions

A groundwater flow and salinity transport model is developed to simulating seawater intrusion in a coastal area with complex hydraulic network in this study. Parameter sensitivity analyses are applied to study the importance of different hydrogeology conditions in seawater intrusion costal aquifers processes.

Form the results of groundwater flow and salinity intrusion model, The abstraction of groundwater as the main water supply source is limited in the fresh lenses. Overexploitation of groundwater in recent years caused groundwater levels continuously to decline and saline groundwater is distributed in many of the areas of Tra Vinh province. The freshwater supply is in shortage for domestic and industries because of salinity intrusion.

In the other hand, abstraction of groundwater is continuously increasing from 2006 to 2017 as the groundwater recharge rate is less than the abstraction rate in the same period. It cause groundwater levels and groundwater storage to decrease rapidly. Seawater intrusion in aquifers happens in many areas of Tra Vinh province. The aquifers most effected happen in the top Holocene aquifer as an important source to provide fresh groundwater by abstraction wells. Seawater intrusion caused total dissolved solid to exceed the standards for domestic and industries water in groundwater. So control of groundwater abstraction has to be considered.

Overall, groundwater head and tot dissolved solid are important observation parameters to seawater intrusion simulation. Hydrological parameters of the groundwater flow and saline transport system are also important to simulations in the costal aquifer and groundwater abstraction systems. The parameter sensitives analysis indicates that simulations of salinity intrusion in costal aquifers can be advantageous to understand groundwater hydrogeological conditions, and play an important role in model calibrations.

Hydraulic conductivity, specific storage and boundary conductance are important hydrological parameters for this model. The output of groundwater levels, change of storage and boundary inflows in the model were used to conduct a sensitivity analysis of the hydraulic conductivity, specific storage and boundary conductance. Some significant conclusions for parameter sensitives are summarized, Different outputs have different sensitivities with the same changes of the values of the parameters. With the use of a head-dependent boundary, groundwater levels are most sensitive in case of a decrease of 50% of hydraulic conductivity, boundary inflow is most sensitive in case of a decrease of 50% of boundary conductance and specific storage coefficient is more sensitive parameters for change of storage.

The constructed groundwater flow and salinity transport model are useful to simulate groundwater hydraulic processes. But there are also a few limitations in the model, which includes (1) insufficient data (2) uncertain parameters

Overexploitation of groundwater is the major reason of salinity intrusion. Reduced abstraction of groundwater is an effective method to mitigate seawater flow into costal aquifers in Tra Vinh province. It is suitable alternative to store rainwater in containers for living and irrigation instead of groundwater abstraction, which can be carried out in Tra Vinh. Since recharge in sandy areas is more effective than clay areas, it is a good strategy to increase recharge in sandy areas through infiltration trenches, road side infiltration trenches in cities and contour farming and trench in farmlands.

References

Shoemaker, W. B. (2004). Important observations and parameters for a salt water intrusion model. *Ground Water*, *42*(6), 829-840.

Razavi, S., & Gupta, H. V. (2015). What do we mean by sensitivity analysis? The need for comprehensive characterization of “global” sensitivity in E arth and E nvironmental systems models. *Water Resources Research*, *51*(5), 3070-3092.McDonald, M. G. and A. W. Harbaugh (1988). A modular three-dimensional finite-difference ground-water flow model, US Geological Survey.

Pannell, D. J. (1997). "Sensitivity analysis of normative economic models: theoretical framework and practical strategies." Agricultural economics **16**(2): 139-152.

Saltelli, A., et al. (2008). Global sensitivity analysis: the primer, John Wiley & Sons.

Aaker, D. A. J. I. . (1995). "Strategic Market Management. New York: John & Wiley Sons."

Allaire, G. and G. Allaire (2007). Numerical analysis and optimization: an introduction to mathematical modelling and numerical simulation, Oxford university press.

Aloysius, N. R., J. Sheffield, J. E. Saiers, H. Li and E. F. J. J. o. G. R. A. Wood (2016). "Evaluation of historical and future simulations of precipitation and temperature in central Africa from CMIP5 climate models." **121**(1): 130-152.

Anderson, M. P., W. W. Woessner and R. J. Hunt (2015). Applied groundwater modeling: simulation of flow and advective transport, Academic press.

Bea, F. and J. J. S. U. Haas "Strategisches Management (4. Aufl., 2005)."

Bui, D. D., N. C. Nguyen, N. T. Bui, A. T. Le, D. T. J. J. o. G. S. Le and Engineering (2017). "Climate change and groundwater resources in Mekong Delta, Vietnam." **5**(1): 76-90.

Chiem, N. H. J. J. J. o. S. A. S. (1993). "Geo-pedological study of the Mekong Delta." **31**(2): 158-186.

Coleman, J. M. and H. Roberts (1989). Deltaic coastal wetlands. Coastal Lowlands, Springer**:** 1-24.

Coulibaly, P., Y. B. Dibike and F. J. J. o. H. Anctil (2005). "Downscaling precipitation and temperature with temporal neural networks." **6**(4): 483-496.

Dang, V. H., D. D. Tran, T. B. T. Pham, D. N. Khoi, P. H. Tran and N. T. J. W. Nguyen (2019). "Exploring Freshwater Regimes and Impact Factors in the Coastal Estuaries of the Vietnamese Mekong Delta." **11**(4): 782.

Danh, V. T. (2008). Household switching behavior in the use of ground water in the Mekong Delta, Vietnam, EEPSEA, IDRC Regional Office for Southeast and East Asia, Singapore, SG.

Doan, Q. T., C. D. Nguyen, Y. C. Chen and K. M. J. L. T. I. Pawan (2014). "Modeling the influence of river flow and salinity intrusion in the Mekong River Estuary, Vietnam." **16**(1): 14-25.

Flood, J. F. and L. B. J. J. o. C. R. Cahoon (2011). "Risks to coastal wastewater collection systems from sea-level rise and climate change." **27**(4): 652-660.

Forster, P., V. Ramaswamy, P. Artaxo, T. Berntsen, R. Betts, D. W. Fahey, J. Haywood, J. Lean, D. C. Lowe and G. Myhre (2007). Changes in atmospheric constituents and in radiative forcing. Chapter 2. Climate Change 2007. The Physical Science Basis.

Greca, I. M. and M. A. J. S. e. Moreira (2002). "Mental, physical, and mathematical models in the teaching and learning of physics." **86**(1): 106-121.

Green, T. R. (2016). Linking climate change and groundwater. Integrated groundwater management, Springer, Cham**:** 97-141.

Guo, W. and G. D. Bennett (1998). Simulation of saline/fresh water flows using MODFLOW. MODFLOW 98 Conference, Golden, CO. In: Poeter, E. et al.(Ed.), 1998 Proceedings (1).

Ha, K., N. T. M. Ngoc, E. Lee and R. Jayakumar (2015). Current status and issues of groundwater in the Mekong river basin, Korea Institute of Geoscience and Mineral Resources (KIGAM).

Herrera-Pantoja, M. and K. J. H. P. A. I. J. Hiscock (2008). "The effects of climate change on potential groundwater recharge in Great Britain." **22**(1): 73-86.

Hewitson, B. and R. G. J. I. J. o. C. A. J. o. t. R. M. S. Crane (2006). "Consensus between GCM climate change projections with empirical downscaling: precipitation downscaling over South Africa." **26**(10): 1315-1337.

Hoc, B., P. K. Huy and H. M. J. J. G. B. Thao (2005). "Groundwater management in Vietnam." **25**: 24-33.

Janardhanan, S. (2012). Integrated multi-objective management of saltwater intrusion in coastal aquifers using coupled simulation-optimisation and monitoring feedback information, James Cook University.

Jing, L. J. I. J. o. R. M. and M. Sciences (2003). "A review of techniques, advances and outstanding issues in numerical modelling for rock mechanics and rock engineering." **40**(3): 283-353.

Kinzelbach, W. J. D. i. W. S. (1986). "Groundwater modelling." **25**.

Lindgren, M. and H. Bandhold (2003). Scenario planning, Springer.

McDonald, M. G. and A. W. Harbaugh (1988). A modular three-dimensional finite-difference ground-water flow model, US Geological Survey.

McDonald, M. G. and A. W. Harbaugh (1988). A modular three-dimensional finite-difference ground-water flow model, US Geological Survey Reston, VA.

McLusky, D. S. and M. Elliott (2004). The estuarine ecosystem: ecology, threats and management, OUP Oxford.

Michael, H. A., V. E. Post, A. M. Wilson and A. D. J. W. R. R. Werner (2017). "Science, society, and the coastal groundwater squeeze." **53**(4): 2610-2617.

Minh, H. V. T., T. V. Tỷ, L. V. Thịnh, T. T. T. Đăng, N. T. T. D. và Lê and T. Y. J. T. c. K. h. T. Đ. h. C. T. Nhi (2014). "Hiện Trạng Khai Thác, Sử Dụng Nước DƯới Đất Ở Vĩnh Châu, Sóc Trăng." 48-58.

Montagna, P. A., T. A. Palmer and J. B. Pollack (2013). Conceptual model of estuary ecosystems. Hydrological changes and estuarine dynamics, Springer**:** 5-21.

Nguyen, A. L., V. H. Dang, R. H. Bosma, J. A. Verreth, R. Leemans and S. S. J. A. De Silva (2014). "Simulated impacts of climate change on current farming locations of striped catfish (Pangasianodon hypophthalmus; Sauvage) in the Mekong Delta, Vietnam." **43**(8): 1059-1068.

Nguyen, K.-A., Y.-A. Liou, H.-P. Tran, P.-P. Hoang, T.-H. J. P. i. E. Nguyen and P. Science (2020). "Soil salinity assessment by using near-infrared channel and Vegetation Soil Salinity Index derived from Landsat 8 OLI data: a case study in the Tra Vinh Province, Mekong Delta, Vietnam." **7**(1): 1-16.

Nguyễn, T. (2011). "Các giải pháp của ngân hàng nhà nước nhằm triển khai nghị quyết 11/NQ-CP ngày 24/02/2011 về kiềm chế lạm phát, ổn định kinh tế vĩ mô, đảm bảo an sinh xã hội."

Nguyen, V. L., T. K. O. Ta and M. J. J. o. A. E. S. Tateishi (2000). "Late Holocene depositional environments and coastal evolution of the Mekong River Delta, Southern Vietnam." **18**(4): 427-439.

Post, V. E. A. and A. D. Werner (2017). "Coastal aquifers: Scientific advances in the face of global environmental challenges."

Post, V. J. H. J. (2005). "Fresh and saline groundwater interaction in coastal aquifers: is our technology ready for the problems ahead?" **13**(1): 120-123.

Postma, D., F. Larsen, N. T. M. Hue, M. T. Duc, P. H. Viet, P. Q. Nhan and S. J. G. e. C. A. Jessen (2007). "Arsenic in groundwater of the Red River floodplain, Vietnam: controlling geochemical processes and reactive transport modeling." **71**(21): 5054-5071.

Spaniol, M. J., N. J. J. F. Rowland and F. Science (2019). "Defining scenario." **1**(1): e3.

Stagars, M. (2016). Data Quality Analysis of Group B: Thailand, Vietnam, and Brunei. Data Quality in Southeast Asia, Springer**:** 87-126.

Thu, P. M., J. J. E. Populus, Coastal and S. Science (2007). "Status and changes of mangrove forest in Mekong Delta: Case study in Tra Vinh, Vietnam." **71**(1-2): 98-109.

Unsal, B., O. Yagbasan and H. J. E. e. s. Yazicigil (2014). "Assessing the impacts of climate change on sustainable management of coastal aquifers." **72**(6): 2183-2193.

Van Hiep, H., N. T. Hung and P. Van Long (2018). Evaluating the Saltwater Intrusion to Aquifer Upper-Middle Pleistocene (qp2–3) in Coastal Area of Tra Vinh Province Due to Groundwater Exploitation. Proceedings of the International Conference on Advances in Computational Mechanics 2017**:** 675-690.

Van, T. P. (2017). "<estimation of groundwater use pattern and distribution in the coastal mekong delta,.pdf>."

Ve, N. B., V.-T. J. U. o. C. T. Anh and B. Project (1990). "Soil Map of the Mekong Delta 1: 250,000 scale based on USDA system."

Vengadesan, M. and E. Lakshmanan (2019). Management of coastal groundwater resources. Coastal Management, Elsevier**:** 383-397.

Vermeulen, P., N. H. Quan, N. D. G. Nam, P. Van Hungd, N. T. Tungd, T. V. Thanhe and R. Dam (2013). Groundwater modeling for the Mekong Delta using iMOD. 20th International Congress on Modelling and Simulation, Adelaide, Australia.

Wagner, F., V. B. Tran and F. G. Renaud (2012). Groundwater resources in the Mekong Delta: availability, utilization and risks. The Mekong Delta System, Springer**:** 201-220.

Werner, A. D., M. Bakker, V. E. Post, A. Vandenbohede, C. Lu, B. Ataie-Ashtiani, C. T. Simmons and D. A. J. A. i. w. r. Barry (2013). "Seawater intrusion processes, investigation and management: recent advances and future challenges." **51**: 3-26.

Wolanski, E. and M. Elliott (2015). Estuarine ecohydrology: an introduction, Elsevier.

Zheng, C. and P. P. Wang (1999). MT3DMS: a modular three-dimensional multispecies transport model for simulation of advection, dispersion, and chemical reactions of contaminants in groundwater systems; documentation and user's guide, Alabama Univ University.

Tables

Table 1 Name and location of observation wells

Name	Aquifers	Layers
Q07701A	Holocene (qh)	Layer 1
Q07701H		
Q217010		
Q404020	Upper Pleistocene (qp_3)	Layer 4
Q40403T	Upper-Middle Pleistocene (qp_{2-3})	Layer 7
Q217020		
Q217030	Middle Pliocene (n_{22})	Layer 13
Q40403Z		
Q406040		
Q2017040	Lower Pliocene (n_{21})	Layer 16
Q40404T		
Q405050M1		
Q021050	Upper Miocene (n_{13})	Layer 19

Table 2 Linkages between conceptual model coverage and MODFLOW

Conceptual model components		GMS coverage	MODFLOW package
Hydrogeological structure	Top elevations	2D scatter points	Layer property package (LPF)
	Bottom elevations	2D scatter points	
	Hydrogeological parameters	19 later coverages	
Boundary conditions	Lateral boundaries	Head-dependent flow coverage	General Head Boundary (GHB) package
	Coastal line	Head-dependent flow coverage or constant head boundary coverage	
Hydrological stresses	Recharge	Area recharge coverage	Recharge (RCH) package
	Rivers	River source coverage	River (RIV) package
	Abstractions	Abstraction sink coverage	Well (WEL) package
Observations	Observation wells	Observation coverage	

Table 3 Difference between previous and new data of K values changed to 0.5 K and 1.5 K

well number	0.5K0	k0	1.5k0	Different with 1.5k0		Different with 0.5k0	
	mean	mean	mean	mean	standard Deviation	mean	standard Deviation
Q07701A	-0.05	-0.49	-0.85	-0.35	0.05	0.45	0.19
Q07701H	-0.52	-0.87	-1.07	-0.19	0.02	0.35	0.18
Q217010	-0.83	-1.15	-1.20	-0.05	0.03	0.32	0.17
Q404020	-11.84	-8.22	-6.62	1.59	0.46	-3.62	1.07
Q40403T	-13.74	-9.18	-7.25	1.94	0.56	-4.56	1.40
Q217020	-11.65	-7.62	-5.94	1.68	0.50	-4.04	1.35
Q271030	-10.61	-7.42	-5.95	1.47	0.58	-3.19	1.57
Q40403Z	-11.63	-8.17	-6.57	1.60	0.55	-3.46	1.40
Q406040	-10.64	-7.47	-6.01	1.46	0.54	-3.18	1.42
Q2017040	-10.42	-7.38	-5.94	1.44	0.59	-3.04	1.57
Q40404T	-11.27	-8.00	-6.46	1.54	0.56	-3.26	1.41
Q405050M1	-11.08	-7.82	-6.30	1.53	0.58	-3.26	1.52
Q021050	-8.77	-6.98	-5.85	1.13	0.60	-1.80	1.36

Table 4 Boundary inflow with different k values

Boundary inflow(m^3/day)					
k_0	$1.5k_0$	$0.5k_0$	Difference with 1.5 k_0	Difference with 0.5 k_0	
Mean	66480.28	75129.91	66504.99	8649.63	24.71
Standard Deviation	7937.49	9043.61	9281.65	3942.45	2727.47

Table 5 Mean and SD change of storage with different k values

change of storage (m^3/day)					
k_0	$1.5k_0$	$0.5k_0$	Difference with 1.5 k_0	Difference with 0.5 k_0	
Mean	-21740.17	-12923.91	-22820.65	8816.27	-1080.48
Standard Deviation	85563.55	86917.18	84804.83	4105.62	2261.20

Table 6 Mean compute groundwater head and difference between new and previous results in 11 wells with different S_s

well number	0.5Ss0	Ss0	1.5Ss0	different with 1.5Ss0		different with 0.5Ss0	
mean	mean	mean	mean	Standard Deviation	mean	Standard Deviation	
Q07701A	-0,60	-0,49	-0,43	0,06	0,06	-0,11	0,06
Q07701H	-0,96	-0,87	-0,82	0,06	0,07	-0,09	0,06
Q217010	-1,21	-1,15	-1,08	0,07	0,07	-0,06	0,07
Q404020	-8,45	-8,22	-8,05	0,17	0,09	-0,23	0,14
Q40403T	-9,47	-9,18	-8,99	0,19	0,08	-0,29	0,15
Q217020	-7,92	-7,62	-7,39	0,23	0,09	-0,30	0,19
Q217030	-7,80	-7,42	-7,12	0,30	0,10	-0,38	0,19
Q40403Z	-8,51	-8,17	-7,94	0,22	0,08	-0,34	0,14
Q406040	-7,82	-7,47	-7,20	0,27	0,08	-0,35	0,17
Q2017040	-7,78	-7,38	-7,06	0,32	0,10	-0,40	0,20
Q40404T	-8,36	-8,00	-7,76	0,24	0,08	-0,36	0,14
Q405050M1	-8,21	-7,82	-7,54	0,29	0,09	-0,38	0,17
Q021050	-7,52	-6,98	-6,61	0,37	0,10	-0,54	0,18

Table 7 Boundary inflow results with the use of different Ss values and the difference between each situations

boundary inflow(m^3/day)					
	Ss_0	$1.5Ss_0$	$0.5Ss_0$	Difference with 1.5 Ss_0	Difference with 0.5 Ss_0
Mean	66480.28	67016.15	73291.23	535.87	6810.95
Standard Deviation	7937.49	6987.43	6440.41	2187.05	3381.21

Table 8 Change of storage results with different Ss values

change of storage(m3/day)					
	Ss0	1.5 Ss0	0.5 Ss0	Difference with 1.5 Ss0	Difference with 0.5 Ss0
Mean	-21740.18	-21341.72	-14247.92	398.46	7492.27
Standard Deviation	85563.56	86664.03	86498.88	2626.14	3868.92

Table 9 Groundwater head in each stress periods in wells with different C_{ghb0}

well number	0.5 C_{ghb0}	C_{ghb0}	1.5 C_{ghb0}	different with 1.5 C_{ghb0}		different with 0.5 C_{ghb0}	
mean	mean	mean	mean	Standard Deviation	mean	Standard Deviation	
Q07701A	-0.65	-0.49	-0.38	0.11	0.07	-0.16	0.11
Q07701H	-1.04	-0.87	-0.76	0.11	0.07	-0.16	0.11
Q217010	-1.32	-1.15	-1.03	0.12	0.07	-0.17	0.11
Q404020	-8.58	-8.20	-7.96	0.24	0.10	-0.37	0.17
Q40403T	-9.63	-9.17	-8.86	0.30	0.12	-0.47	0.20
Q217020	-8.15	-7.60	-7.22	0.38	0.13	-0.55	0.21
Q217030	-7.92	-7.40	-7.04	0.36	0.14	-0.52	0.22
Q40403Z	-8.69	-8.15	-7.80	0.35	0.14	-0.54	0.22
Q406040	-7.97	-7.45	-7.10	0.35	0.14	-0.52	0.22
Q2017040	-7.87	-7.36	-7.01	0.35	0.14	-0.52	0.22
Q40404T	-8.53	-7.99	-7.63	0.36	0.14	-0.55	0.23
Q405050M1	-8.31	-7.80	-7.47	0.34	0.14	-0.51	0.22
Q021050	-7.55	-6.96	-6.58	0.38	0.16	-0.59	0.27

Table 10 Change of storage results with different Cghb0 values

boundary inflow (m^3/day)					
	C_{ghb0}	1.5 C_{ghb0}	0.5 C_{ghb0}	Difference with 1.5 C_{ghb0}	Difference with 0.5 C_{ghb0}
Mean	66223.73	76521.19	49452.54	10927.27	-16141.32
Standard Deviation	7861.98	9064.43	6133.87	7212.33	7406.10

Table 11 Change of storage results with different Cghb0 values

change of storage (m^3/day)					
	C_{ghb0}	1.5 C_{ghb0}	0.5 C_{ghb0}	Difference with 1.5 C_{ghb0}	Difference with 0.5 C_{ghb0}
Mean	55159.91	56769.43	47547.36	1609.52	-7612.54
Standard Deviation	94496.07	104898.64	84844.72	17637.34	22298.66

Figures

Figure 1

Map of Tra Vinh province (Source: https://vietnamnews.vn/)

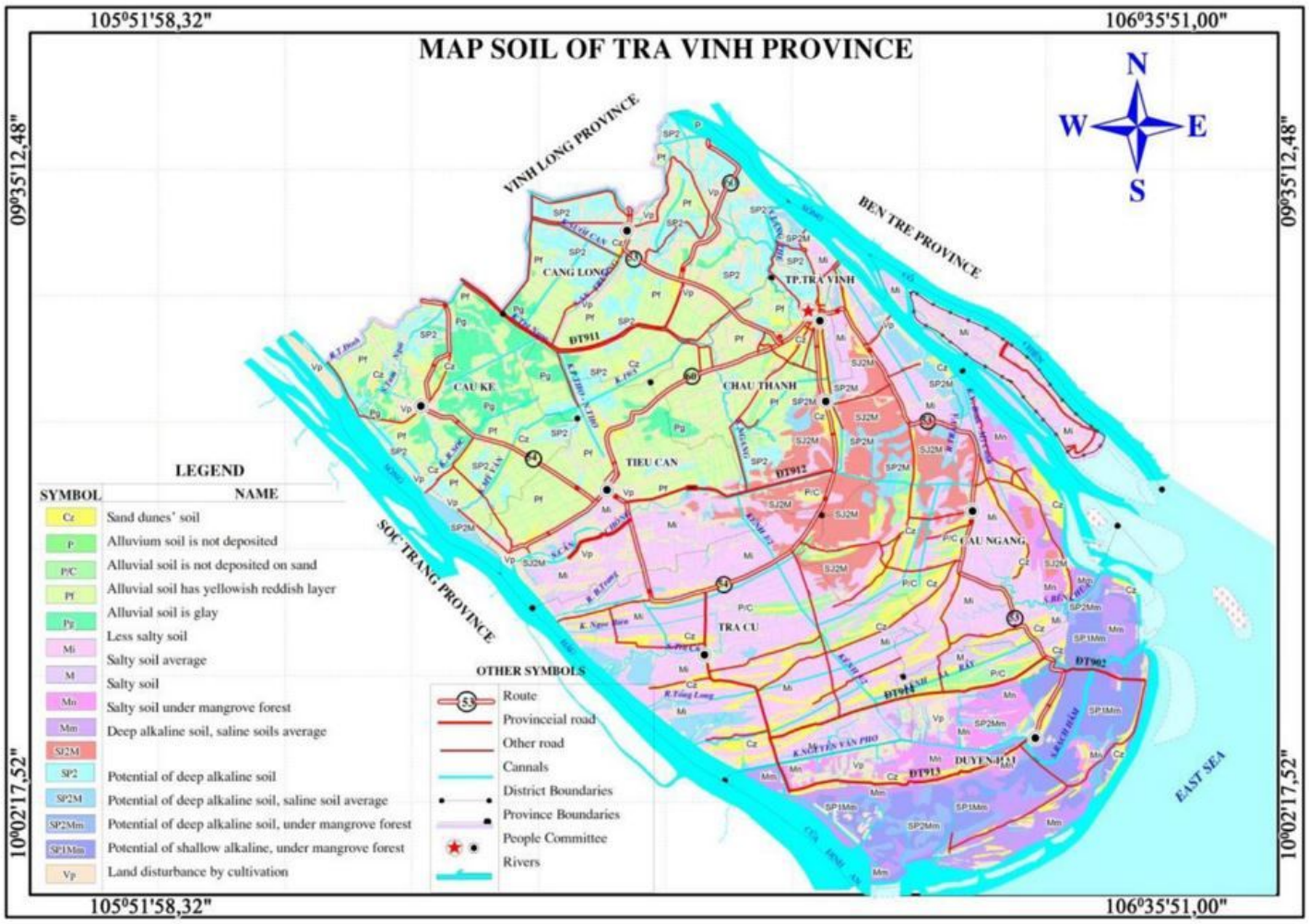

Figure 2

Type of soil map of Tra Vinh (source:(Nguyen 2020))

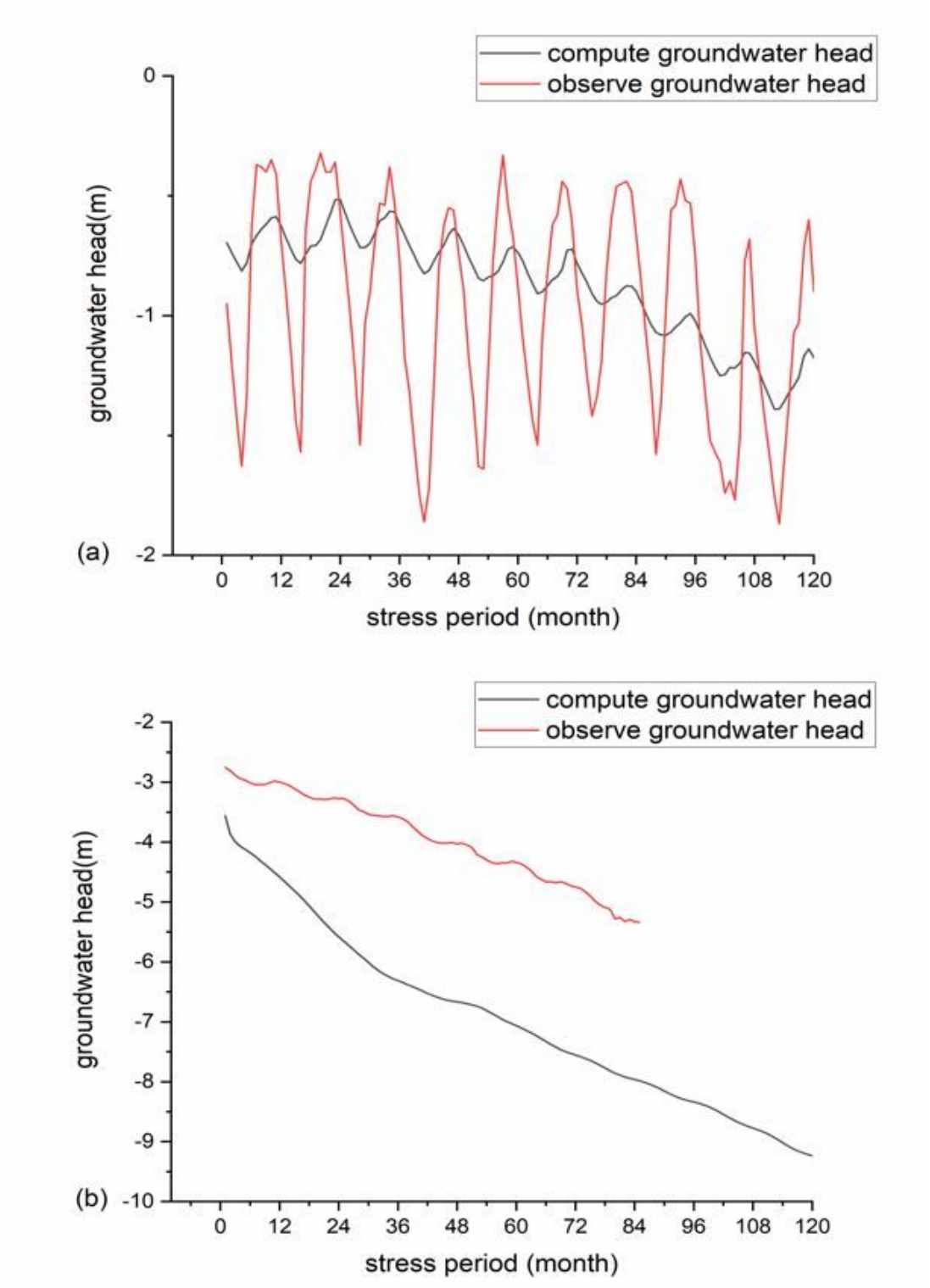

Figure 3

Groundwater head sensitive for k value with well (a) Q07701H (layer 1) and (b) Q021050 (layer 19)

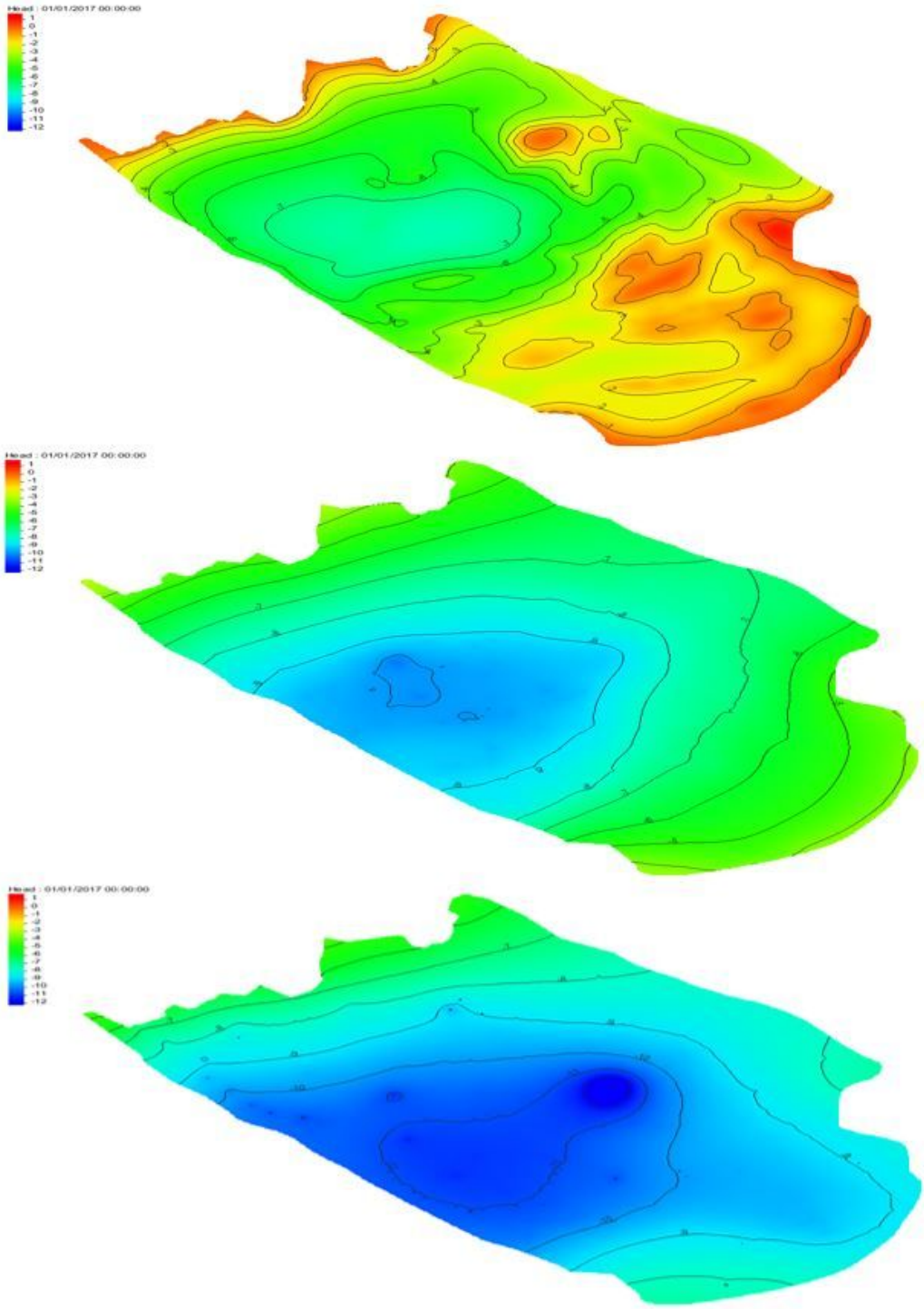

Figure 4

The contour map for groundwater head in (a) layer 1(Holocene (qh)), (b) layer 4 (Upper Pleistocene (qp3)) and (c) layer 7 (Upper-Middle Pleistocene (qp2-3))

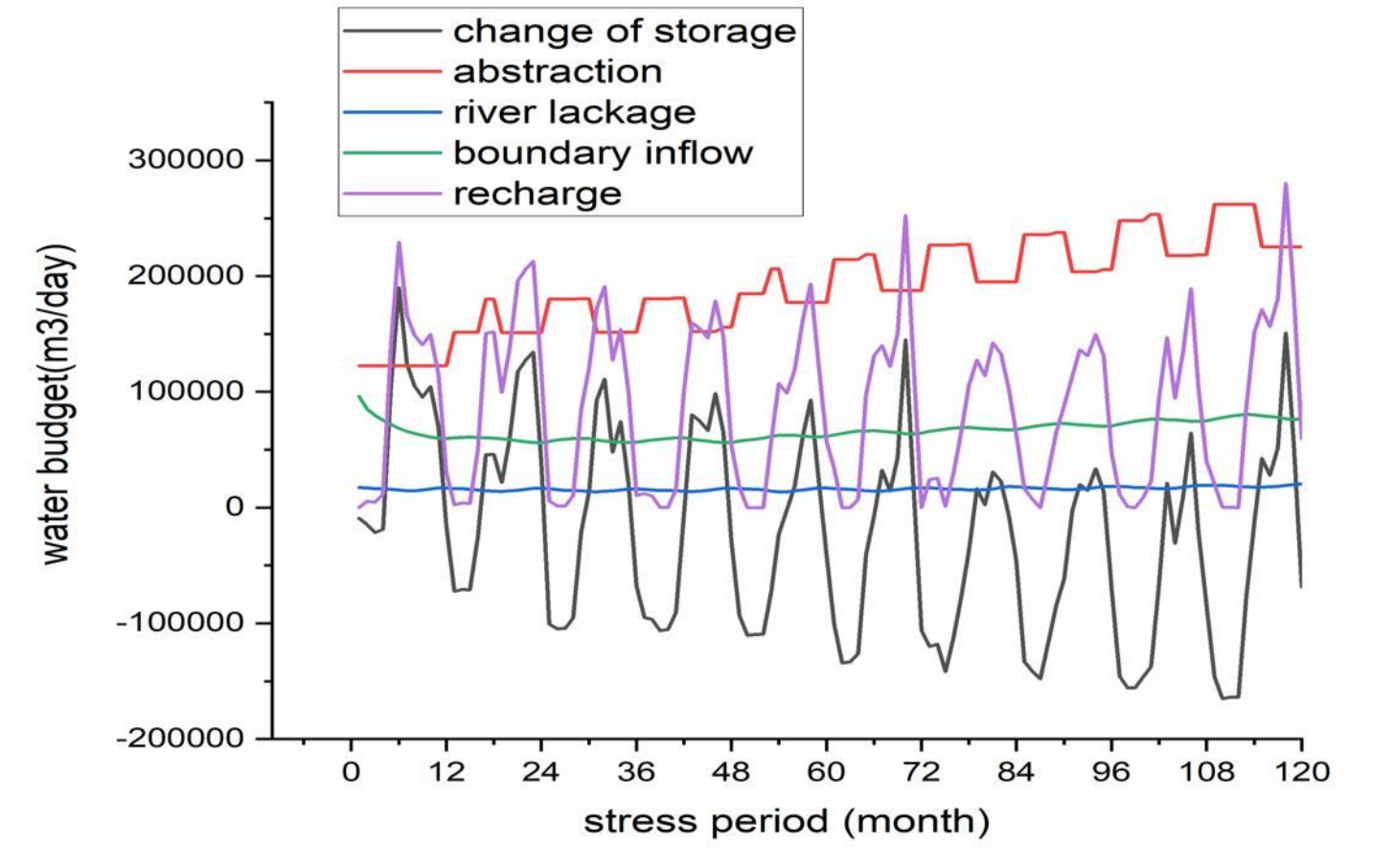

Figure 5

Water budget for whole model

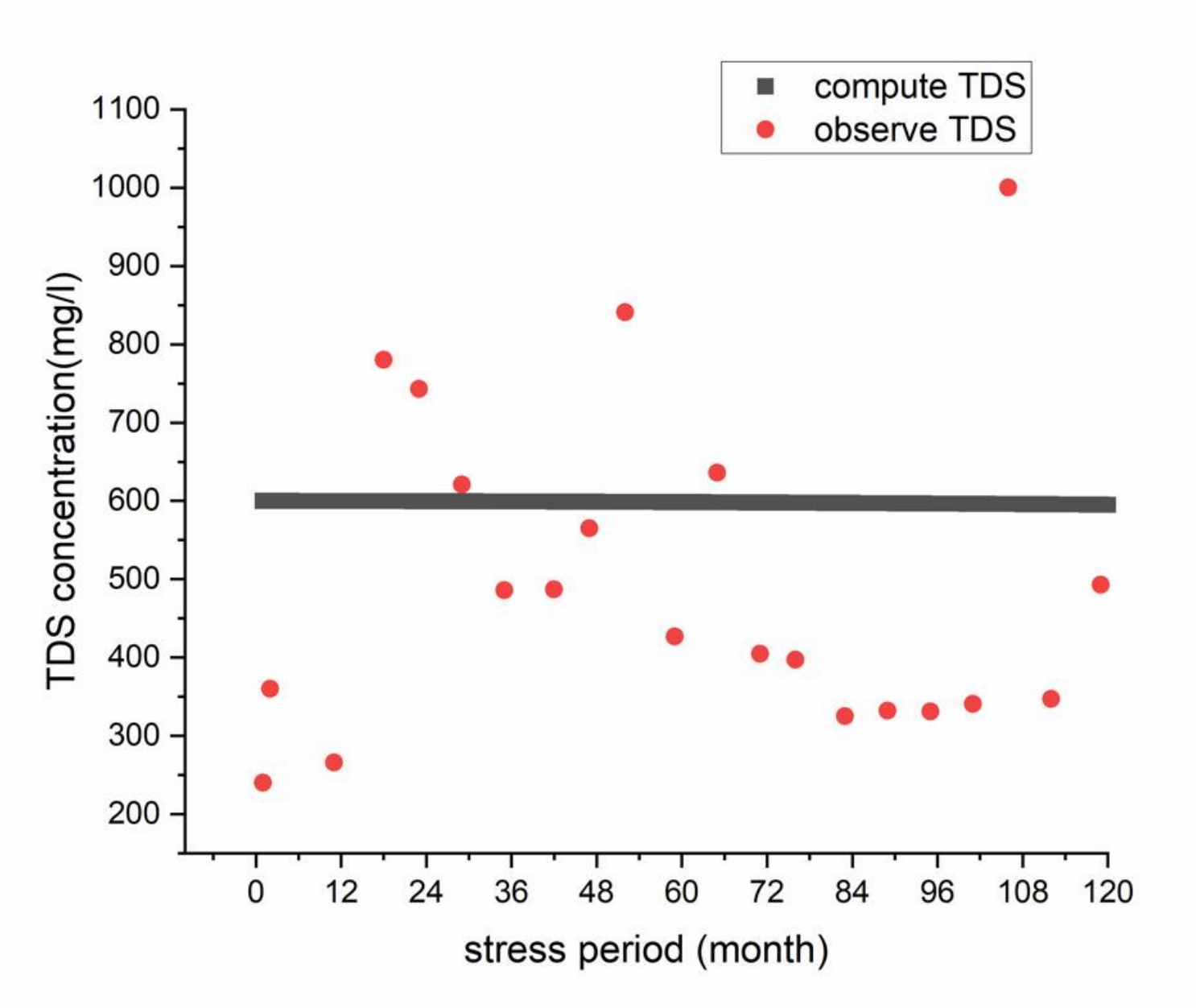

Figure 6

Groundwater TDS concentration value in duration observed wells Q07701H (layer 1)

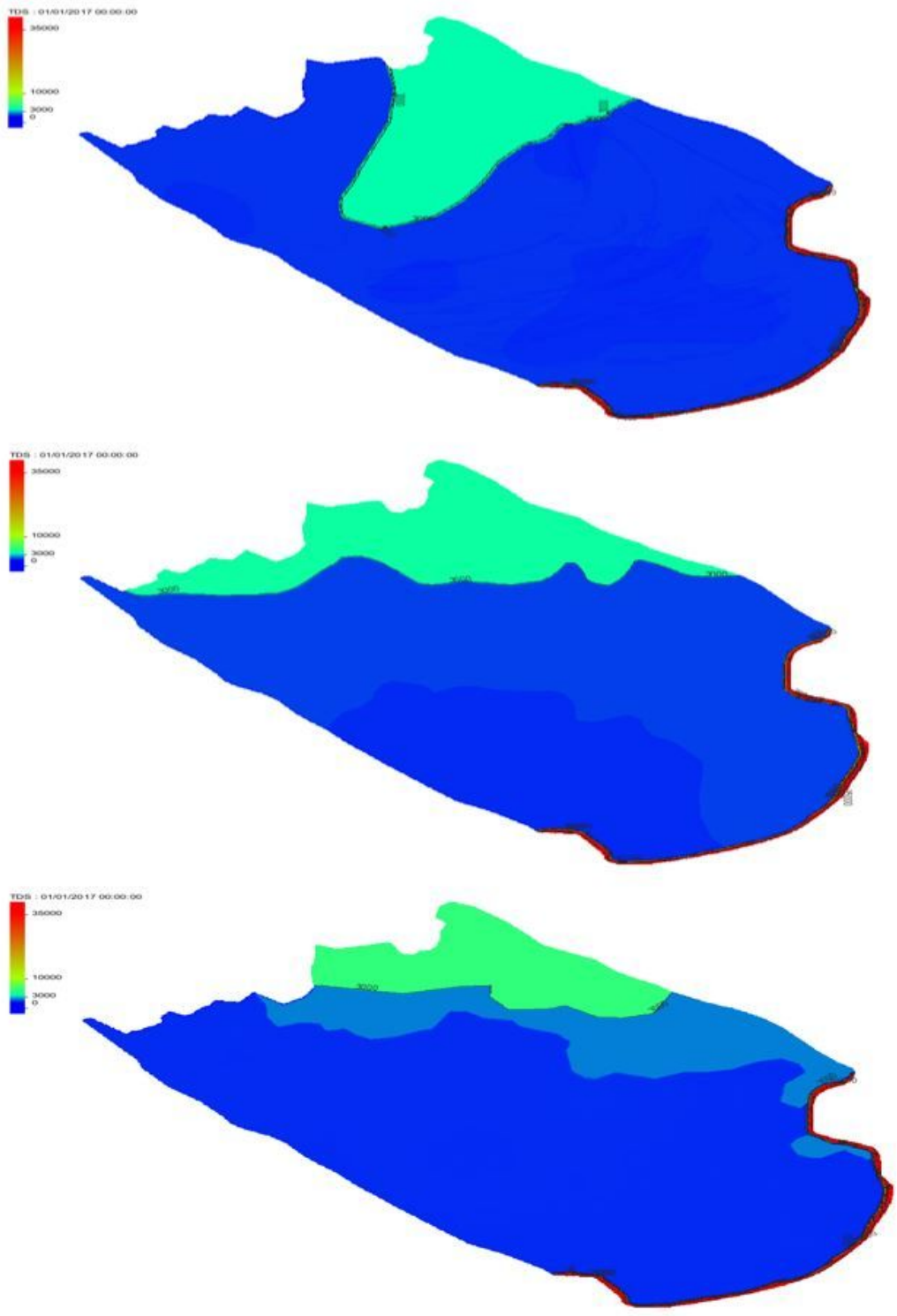

Figure 7

The contour map for total dissolved solid (TDS) in (a) layer1 (Holocene (qh)), (b) layer 4(Upper Pleistocene (qp3)) and (c) layer 7(Upper-Middle Pleistocene (qp2-3))

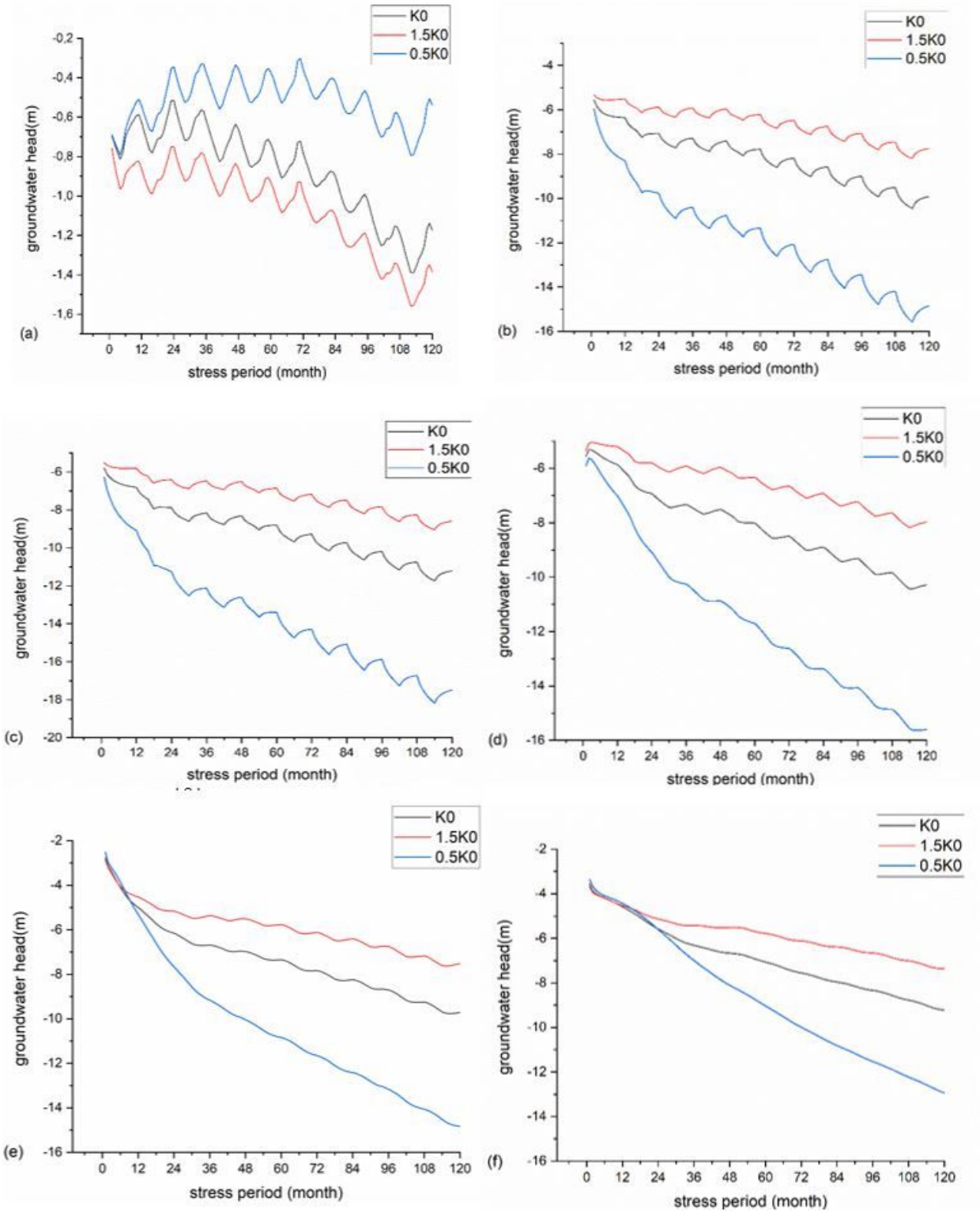

Figure 8

Groundwater head change in different stress periods in wells (a) Q07701H (layer 1), (b) Q404020 (layer 4), (c) Q40403T (layer 7), (d) Q40403Z (layer 13), (e) Q2017040 (layer 16) and (f) Q021050 (layer 19)

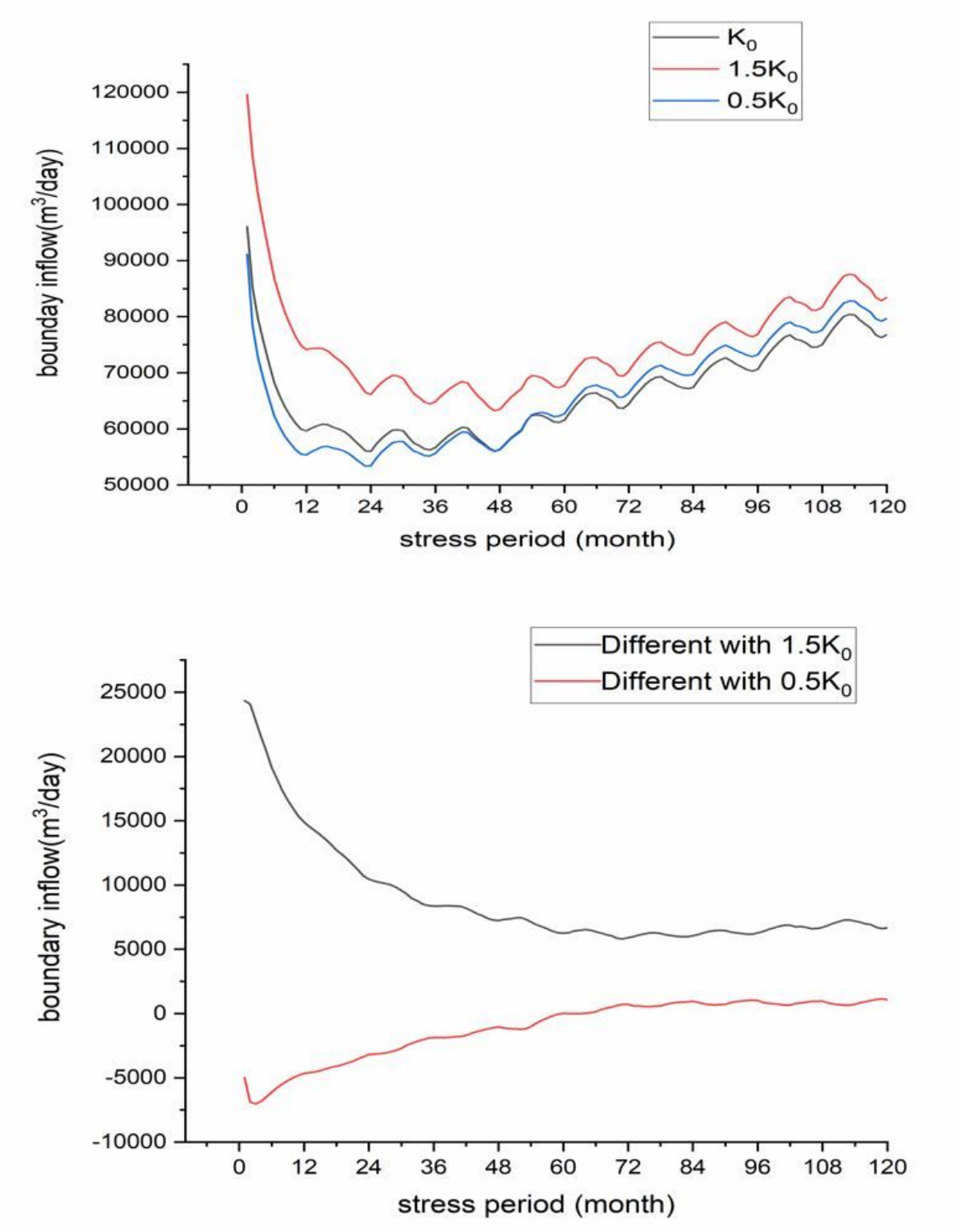

Figure 9

Boundary inflow results in Tra Vinh with the use of different K values

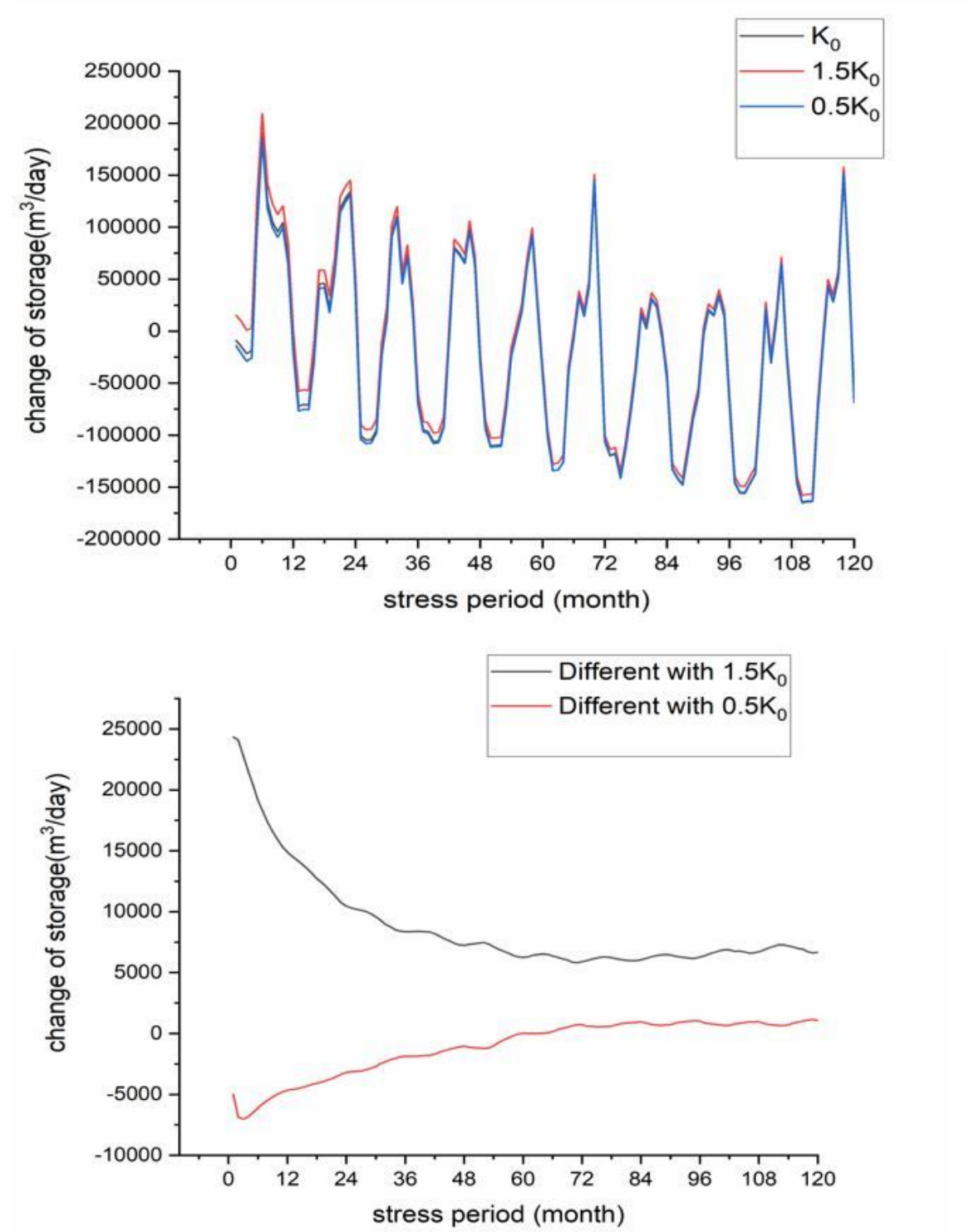

Figure 10

Change of storage sensitive for k value with k, 0.5k and 1.5k

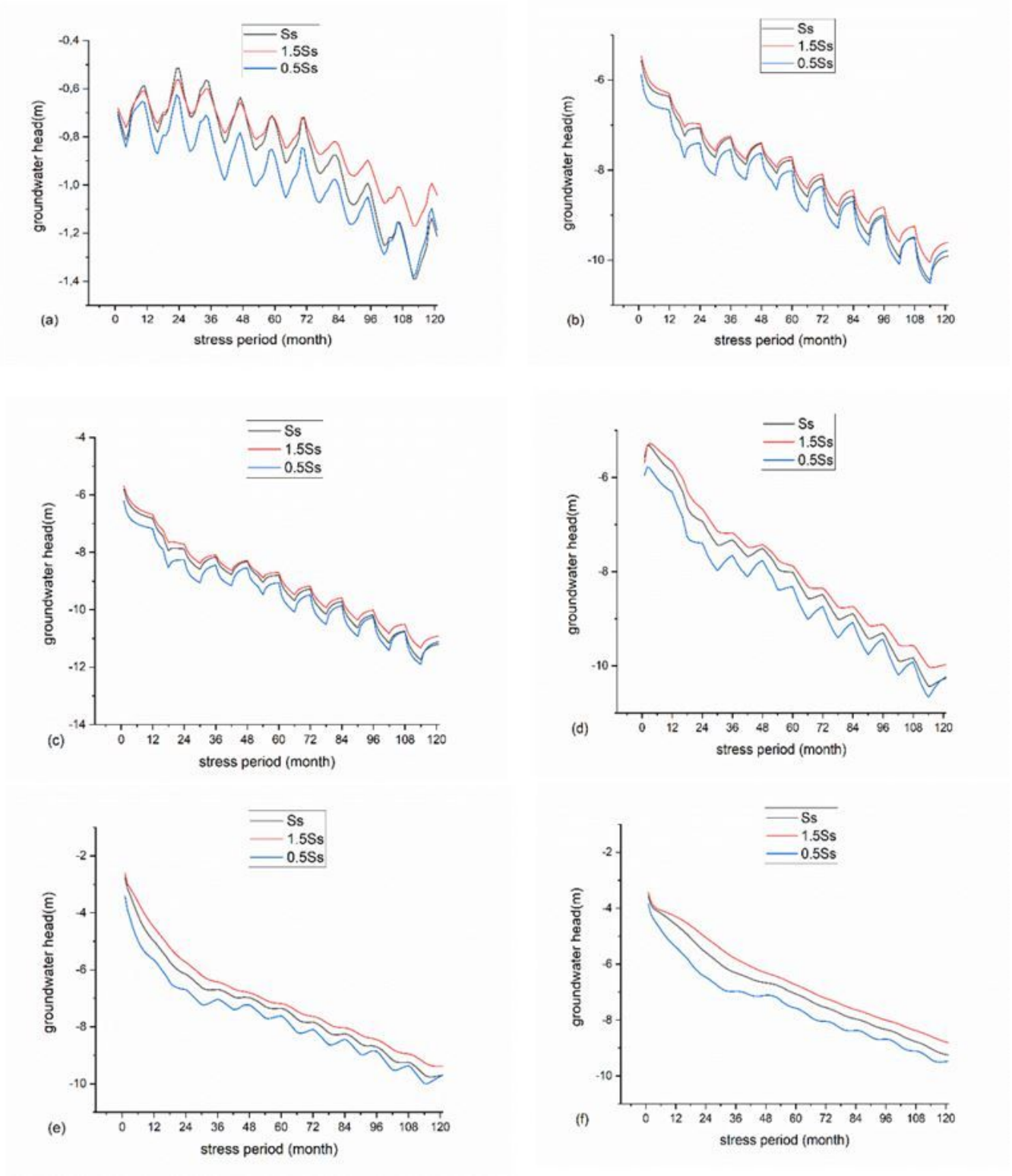

Figure 11

Groundwater head results in each stress periods in well (a) Q07701H (layer 1), (b) Q404020 (layer 4), (c) Q40403T (layer 7), (d) Q40403Z (layer 13), (e) Q2017040 (layer 16) and (f) Q021050 (layer 19)

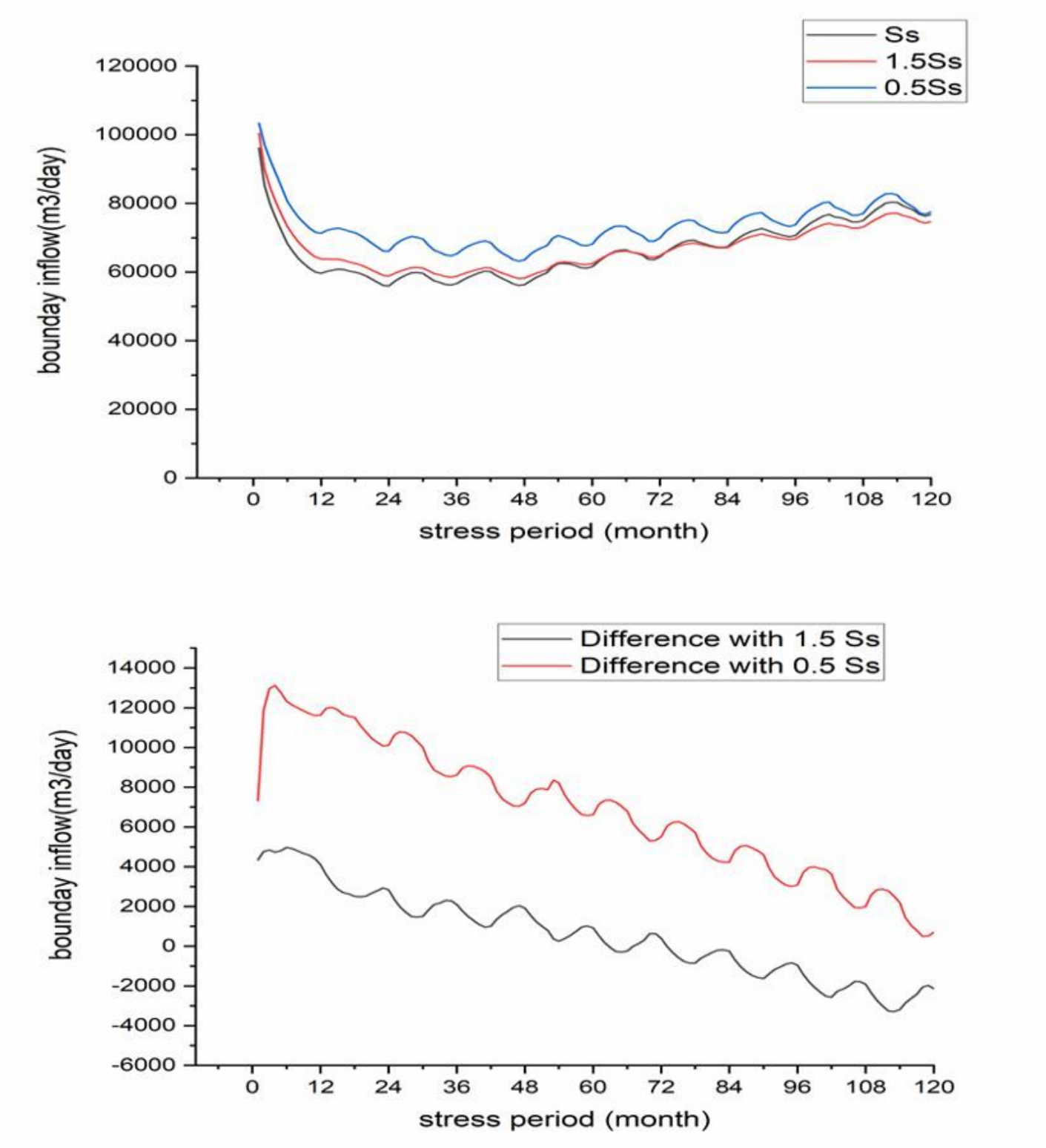

Figure 12

Boundary inflow results with the use of different Ss values

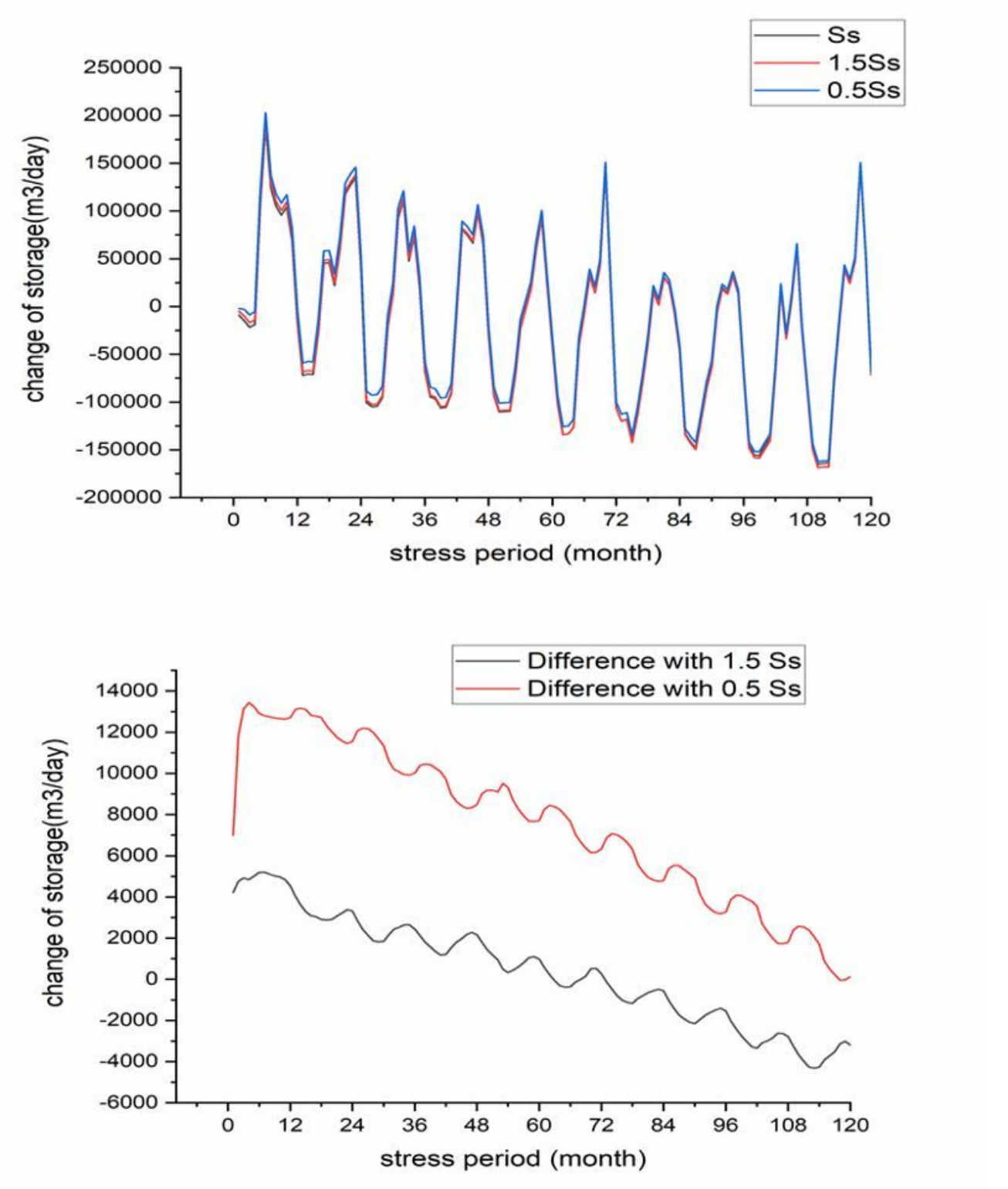

Figure 13

Change of storage results with different Ss values

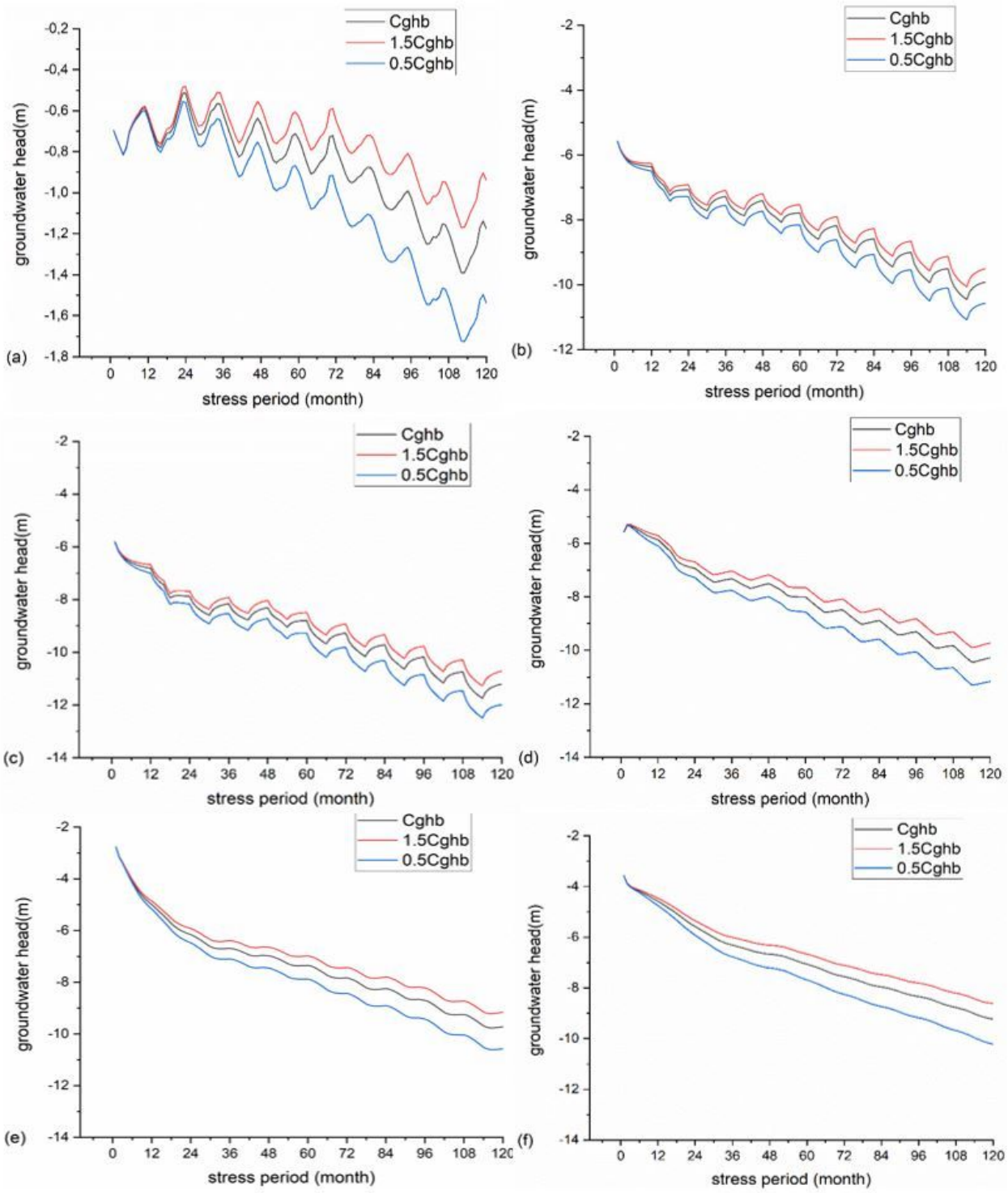

Figure 14

Groundwater head in each stress periods with conductance values in well (a) Q07701H (layer 1), (b) Q404020 (layer 4), (c) Q40403T (layer 7), (d) Q40403Z (layer 13), (e) Q2017040 (layer 16) and (f) Q021050 (layer 19)

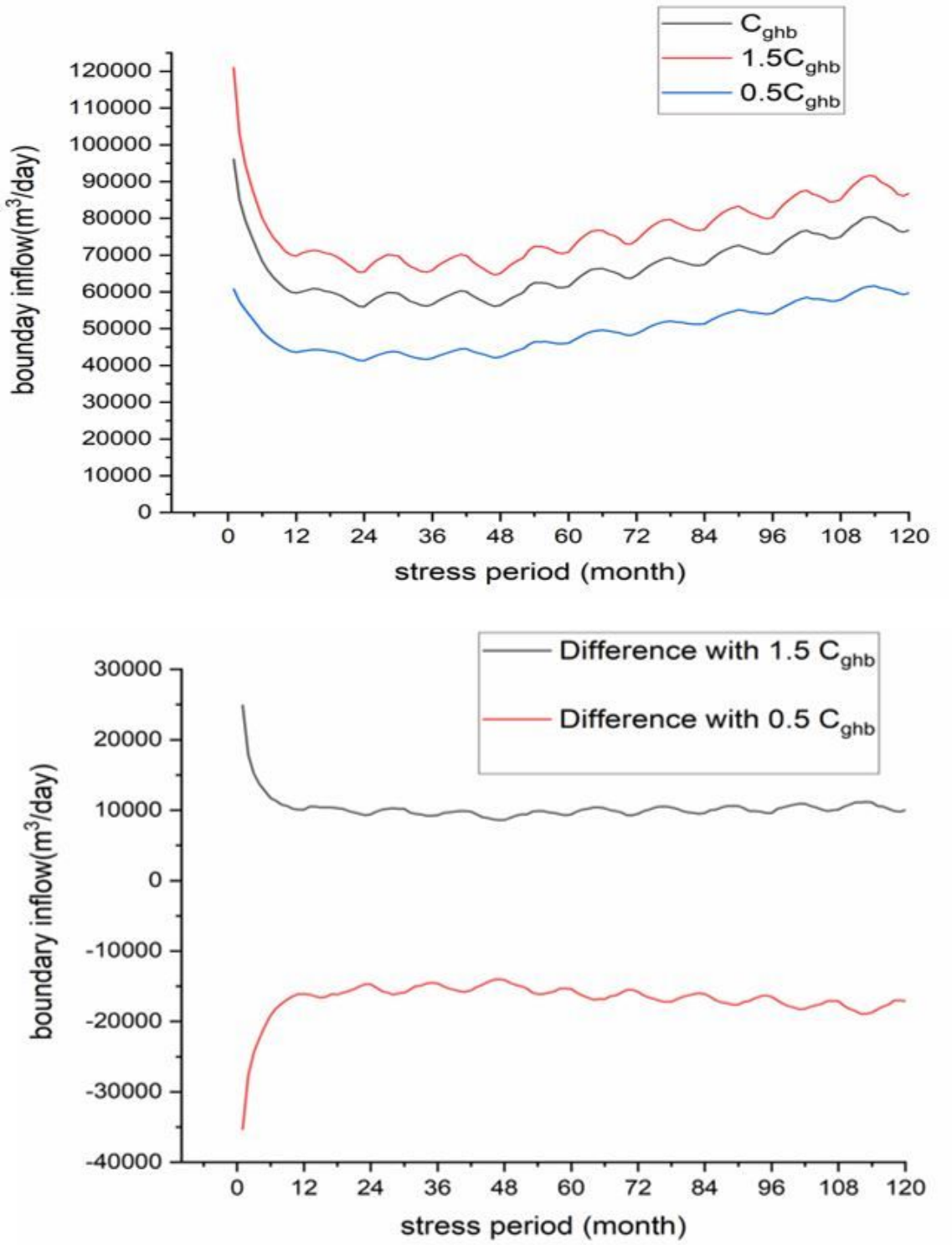

Figure 15

Boundary inflow results with the use of different Cghb0 values

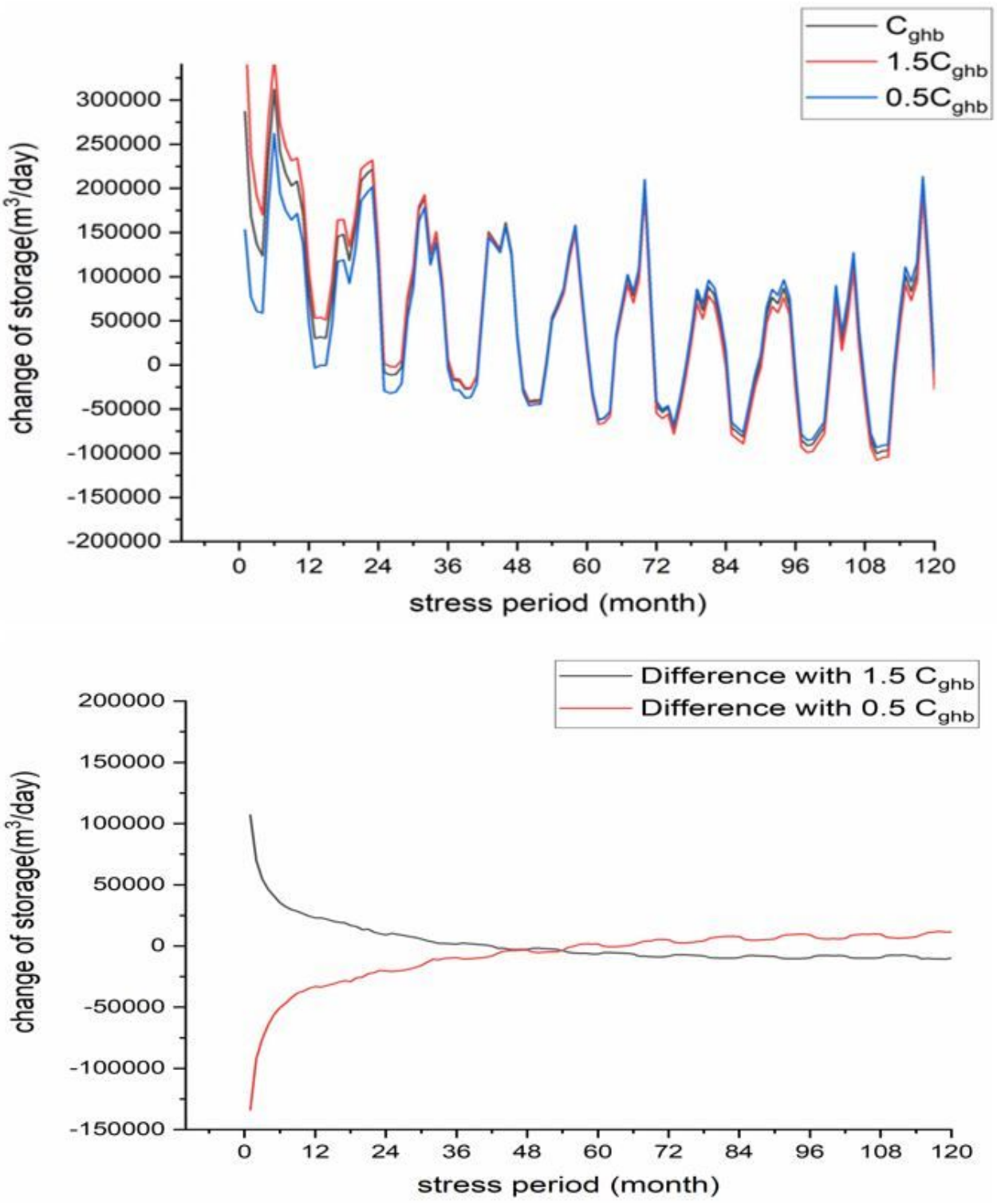

Figure 16

Change of storage results with different Cghb0 values